International Journal of Nanomedicine

Dovepress
open access to scientific and medical research

Open Access Full Text Article

ORIGINAL RESEARCH

Histochemical and biochemical analysis of the size-dependent nanoimmunoresponse in mouse Peyer's patches using fluorescent organosilica particles

This article was published in the following Dove Press journal:
International Journal of Nanomedicine
14 March 2012
Number of times this article has been viewed

Aziz Awaad[1,2]
Michihiro Nakamura[1]
Kazunori Ishimura[1]

[1]Department of Anatomy and Cell Biology, the University of Tokushima Graduate School, Kuramoto, Tokushima, Japan; [2]Department of Zoology, Faculty of Science, Sohag University, Sohag, Egypt

Background/objective: The size-dependent mucosal immunoresponse against nanomaterials (nanoimmunoresponse) is an important approach for mucosal vaccination. In the present work, the size-dependent nanoimmunoresponse of mouse Peyer's patches (PPs) and immunoglobulin A (IgA) level was investigated using fluorescent thiol-organosilica particles.

Methods: Various sizes of fluorescent thiol-organosilica particles (100, 180, 365, 745, and 925 nm in diameter) were administered orally. PPs were analyzed histochemically, and IgA levels in PP homogenates, intestinal secretions around PPs, and bile were analyzed biochemically.

Results: When compared with the larger particles (745 and 925 nm), oral administration of smaller thiol-organosilica particles (100, 180, and 365 nm) increased the number of $CD11b^+$ macrophages and IgA^+ cells in the subepithelial domes of the PPs. Additionally, administration of larger particles induced the expression of alpha-L-fucose and mucosal IgA on the surface of M cells in the follicle-associated epithelia of PPs and increased the number of $33D1^+$ dendritic cells in the subepithelial domes of the PPs. IgA contents in the bile and PP homogenates were high after the administration of the 100 nm particles, but IgA levels in the intestinal secretions were high after the administration of the 925 nm particles. Two size-dependent routes of IgA secretions into the intestinal lumen, the enterohepatic route for smaller particles and the mucosal route for larger particles were proposed.

Conclusion: Thiol-organosilica particles demonstrated size-dependent nanoimmunoresponse after oral administration. The size of the particles may control the mucosal immunity in PPs and were useful in mucosal vaccination approaches.

Keywords: thiol-organosilica particles, Peyer's patches immune cells, IgA, mucosal vaccination

Introduction

Nanoparticles (NPs) have the following advantages for mucosal vaccination: controlled release, specific targeting, and efficient immunization.[1,2] The size-dependent immunoresponse against nanomaterials in various immune tissues (nanoimmunoresponse) is a new and attractive field, and mucosal immunity induction and enhancement using nanomaterials is a nanoimmunoresponse that is important to understand for developing new applications for nanomaterials.

The initiation of adaptive mucosal immunity occurs in organized, mucosal lymphoid tissues such as the Peyer's patches (PPs) of the small intestine.[3] The PP immune cells play an important role in the immune defense against pathogens and antigen-coated NPs.[3,4]

Correspondence: Michihiro Nakamura
Department of Anatomy and Cell Biology, the University of Tokushima Graduate School, 3-18-15 Kuramoto, Tokushima 770-8503, Japan
Tel +81 88 633 9220
Fax +81 88 633 9426
Email michy@basic.med.tokushima-u.ac.jp

submit your manuscript | www.dovepress.com
Dovepress
http://dx.doi.org/10.2147/IJN.S28675

A main immunological function of macrophages is to remove NPs from the body, especially from gut lymphoid tissue or from other organs.[5,6] Additionally, dendritic cells (DCs) have a primary role in the immune defense against mucosal pathogens and antigen-coated NPs and in the uptake of NPs from gut-associated lymphoid tissue.[7,8]

Analysis of the size-dependent nanoimmunoresponses of immune cells in PPs is important for understanding the mucosal immunity. Some previous studies detected a change in the numbers of immune cells in PPs after oral administration of bacteria and viruses such as *Lactobacillus paracasei* and *Cowpea Mosaic* virus.[9–13] But studies on the nanoimmunoresponse, such as those on the change in the number of PP immune cells after oral administration of nanomaterials, are very rare. In a previous study, a powerful intestinal secretagogue and induction of an abnormal mucin composition in the intestinal mucosa were observed after oral administration of silver NPs (average diameter of 60 nm). The silver NPs decreased the number of mucus cells, and mucus was released from the goblet cells in the intestine. Moreover, rectum and colon mucosa exhibited a higher amount of sialomucins.[14] It was also reported that fluorescent polystyrene particles (200 nm) were efficiently transported by M cells to the subepithelial dome (SED) of the PPs and were ingested by $CD11c^+$ cells and that a small number of microparticles were ingested with $CD11b^+$ macrophages after oral administration.[4]

Locally produced immunoglobulin A (IgA) is considered to be among the most important of protective humoral immune factors.[15–17] Recently, mucosal and systemic nanoimmunoresponses after oral administration of particles have been actively investigated.[4,18–20] It has been previously reported that a mucosal nanoimmunoresponse occurred after using functionalized NPs of a single particle size.[2,19–21] Also, intestinal IgA and serum HBsAg-specific total antibodies are specific mucosal nanoimmunoresponses against antigens and have been induced after oral administration of poly lactic-co-glycolic acid (PLGA) microparticles (2–9 μm) plasmid DNA, which encoded HBsAg,[19] and PLGA NPs (390 nm), which encapsulated the hepatitis B surface antigen.[18] Additionally, the IgA, size-dependent nanoimmunoresponse in serum after oral administration of functionalized particles of various sizes has been reported.[22–24] In another study, PLGA NPs (1–5 μm), which encapsulated the hepatitis B surface antigen (HBsAg), induced secretory IgA levels in salivary, intestinal, and vaginal secretions.[25] However, no report has been published on the changes in the numbers of immune cells from PPs that was based on the size-dependent nanoimmunoresponse against NPs. Therefore, studies regarding the size-dependent nanoimmunoresponse against nanomaterials in the gastrointestinal tract require further investigation.

The authors of this present study recently developed new nanomaterials, ie, organosilica particles, for nanomedicine applications.[26–32] Various sizes of fluorescent, thiol-organosilica particles can be synthesized with a narrow size distribution, high dispersion, and unique surface charge.[28] Recently it was reported that thiol-organosilica particles have excellent adhesion ability to mucosal surfaces, possibly due to effects of thiol residue.[33] The authors of this present study previously

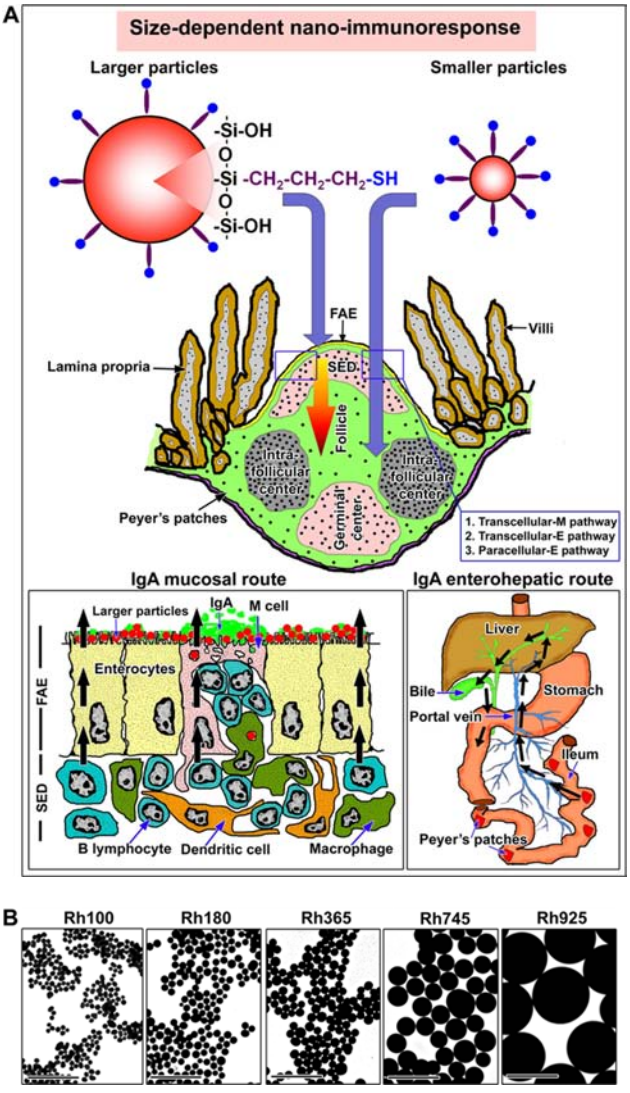

Figure 1 (**A**) Schemes for two size-dependent nanoimmunoresponses induced by smaller thiol-organosilica particles and larger thiol-organosilica particles, and two possible routes, enterohepatic route and mucosal route, of two size-dependent IgA secretions. (**B**) Electron micrograph of different sizes of fluorescent thiol-organosilica particles.
Note: Scale bar = 1 μm.
Abbreviations: FAE, follicle associated epithelium; IgA, immunoglobulin A; paracellular-E pathway, paracellular pathway between enterocytes; Rh, rhodamine B; SED, subepithelial dome; transcellular-E pathway, transcellular pathway through enterocytes; transcellular-M pathway, transcellular pathway through M cell.

administered various sizes of thiol-organosilica particles orally into mice and demonstrated the size-dependent uptake and novel pathways in PP (Figure 1A). In the present study, histochemical studies of PP were performed to quantitatively investigate the size-dependent nanoimmunoresponse enhancement of surface molecules on M cells and the immune cell number. Furthermore, the size-dependent nanoimmunoresponse enhancement of IgA in PP tissue homogenates and in bile and intestinal secretions surrounding the PPs was biochemically investigated. The outcomes from this study could provide important information for enhancing mucosal and systemic immunity against nanomaterials and could improve mucosal vaccination efficiency and nanomedicine applications through intestinal mucosa.

Materials and methods

Materials

3-Mercaptopropyltrimethoxysilane, rhodamine B (Rh), lectin *Ulex europaeus* agglutinin I (UEA I) conjugated with fluorescein isothiocyanate (FITC), and anti-mouse IgA (alpha chain-specific) antibody conjugated with FITC were purchased from Sigma–Aldrich Chemical Co (Saint Louis, MO). Anti-mouse CD11b (Mac 1 alpha chain) antibody and affinity-purified anti-mouse DC marker (33D1) were purchased from eBioscience, Inc (Kobe, Japan). A sheet of polyvinylidene difluoride (PVDF) membrane was obtained from Amersham Pharmacia Biotech UK Limited (Buckinghamshire, England).

Preparation and characterization of thiol-organosilica particles

The particles were prepared from 3-mercaptopropyltrimethoxysilane as the silica source, and five different sizes of particles containing Rh B (100 nm, 180 nm, 365 nm, 745 nm, and 925 nm in diameter) were prepared according to previous methods with slight modification[28,32] (Figure 1B and Table 1). The images of particles were obtained with a Hitachi H7650 electron microscope (Tokyo, Japan), and the sizes and standard deviations of about 200 particles were analyzed by Image-Pro Plus software (Media Cybernetics, Inc, Bethesda, MD).

Table 1 Average sizes with standard deviations and coefficient variants of fluorescent thiol-organosilica particles containing Rh

Thiol-organosilica particles	Average diameter (nm) ± Standard deviation	Coefficient variants (%)
Rh100	97 ± 11	11.3
Rh180	181 ± 21	12.0
Rh365	365 ± 48	13.3
Rh745	745 ± 77	10.4
Rh925	925 ± 133	14.3

Abbreviation: Rh, rhodamine B.

Oral administration of different sizes of thiol-organosilica particles

Female C57 BL/6J mice (6–8 weeks old) were used for this study, and all experiments were conducted according to the guidelines for the Care and Use of Animals that was approved by the Animal Experiments Committee at the University of Tokushima. Before administration of the particles, the mice were fasted for 4 hours with free access to water, and the animals were then separated into six groups (four mice per group). Each group of mice was orally administered 5 mg (100 μL of 50 mg/mL) of various sizes of particles. The control group was orally administered 5 mg (100 μL of 50 mg/mL) of food that had been dissolved in phosphate-buffered saline solution. After oral administration, the mice were left with free access to water. Five to seven PPs were dissected from the intestines of the mice, fixed with 4% paraformaldehyde, and processed for cryostat sectioning.

Immunohistochemical and quantitative analysis of PPs

Sections were incubated with lectin UEA I conjugated with FITC (20 μg/mL), anti-mouse IgA antibody conjugated with FITC (68.75 μg/mL), anti-mouse CD11b antibody (0.625 μg/mL), or anti-mouse 33D1 (5 μg/mL). All sections were observed with an inverted TE 2000 fluorescence microscope (Nikon, Kanagawa, Japan) equipped with a 100 W mercury lamp as a light source and a CCD camera. For quantitative analysis of PP immune cells, about 20 representative sections (n = 20) were selected from each group, and a survey to count IgA^+ cells, $33D1^+$ DCs, and $CD11b^+$ macrophages for each PP SED was performed. The number of PP immune cells was normalized with an averaged area of the PP SED (0.154 mm^2).

Western blotting of PP homogenates, bile, and intestinal secretions IgA

A control and two experimental groups, which were administrated either Rh100 or Rh925, were used for this study. Collected bile from gall bladder and intestinal secretions surrounding PPs and PP tissues were applied to Western blotting. A suitable and equal amount of protein from each sample (5 μg of bile, 15 μg of PP homogenates, and 10 μg of intestinal secretions) was applied to sodium dodecyl

sulfate polyacrylamide gel electrophoresis. Proteins on the gel were transferred to a PVDF membrane using a semi-dry transfer unit electrophoretically. The membrane was incubated with anti-IgA antibody conjugated to FITC (11 μg/mL, 1:100 dilution) for 1 hour, and scanned using a Typhoon scanner 9400 (GE Healthcare, Tokyo, Japan). IgA bands were analyzed using ImageQuant TL software, and the IgA value was calculated from the means ± standard deviations of four mouse groups (n = 4).

Results

Histochemical and immunohistochemical analysis of the nanoimmunoresponse of PPs after oral administration of thiol-organosilica particles

Localization of thiol-organosilica particles with immune cells of PPs

After 4 hours of oral administration, the co-localization of thiol-organosilica particles and some immune cells from PPs was observed. The uptake of thiol-organosilica particles by PPs was size-dependent, ie, the fluorescence area from smaller particles (Rh100, Rh180, and Rh365) in the SEDs of PPs was larger than that from larger particles (Rh745 and Rh925) (Figures 2–5). To identify the precise localization of the particles in the SEDs of the PPs, lectin UEA I labeling of follicle-associated epithelium (FAE) M cells, and immunohistochemical staining of macrophages, DCs, and IgA$^+$ cells were performed. As shown in Figure 2A, PP FAE contains UEA I$^-$ enterocytes and UEA I$^+$ M cells that are scattered between enterocytes. UEA I$^+$ M cells expressed an alpha-L-fucose residue only on the surface and upper cytoplasm of the cells (Figure 2A, arrowheads). Only a few of the smaller particles were localized with the green fluorescence that represented UEA I (Figure 2C and D); however, for the larger particles, nearly all red fluorescence from the particles was observed to localize with the green fluorescence of UEA I (Figure 2F). The particles localized on the surface and in the cytoplasm of UEA I$^+$ M cells, but they were then translocated into the SEDs of the PPs. Immunohistochemical staining with a CD11b antibody, a specific marker for macrophages, revealed that CD11b$^+$ macrophages (Figure 3A, arrowheads) were scattered in the SEDs of the PPs of the control. As shown in Figure 3B–D, CD11b$^+$ macrophages with smaller particles (Rh100, Rh180, and Rh365) fluoresced more than those with larger particles (Rh745 and Rh925) (Figure 3E and F). In some cases, the particles diffused freely into the SED of the PPs or into intercellular spaces, as shown by fluorescence (Figures 3C, D, and 5A) and electron microscopy (Supplementary figures 1 and 2). Histochemically, to identify DCs and IgA$^+$ cells in PPs, 33D1 and IgA antibodies (Figure 4A, arrowheads; Figure 6A, bold arrows) were used, respectively. A small number of particles co-localized with 33D1$^+$ DCs, compared with CD11b$^+$ macrophages (Figure 4B, bold arrows), and in some cases, a small amount of particles co-localized with 33D1$^+$ DCs (Figure 5B, arrowheads). Furthermore, co-localization of particles and IgA$^+$ cells (Figure 6B, arrowheads) was rare. These data revealed that a main role of UEA I$^+$ M cells and CD11b$^+$ macrophages is to take up particles into the SEDs of PPs.

Nanoimmunoresponse of immune cells of PPs after oral administration of thiol-organosilica particles

In contrast to the M cells from the PPs of the control group (Figure 2A, arrowheads), the smaller particles (Rh100, Rh180, and Rh365) increased the expression of alpha-L-fucose residue on the surface of M cells and redistributed it into the cytoplasm and the apical region of the cells (Figure 2B–D). However, uptake and mechanical adhesion of the larger particles (Rh745 and Rh925) (Figure 2E and F) with the FAE and M cells of PPs increased the expression of alpha-L-fucose residue and redistributed it to the apical region of the cell, in contrast to what occurred with smaller particles (Rh100, Rh180, and Rh365) and M cells from the PPs of the control group. Additionally, electron microscopy analysis showed that mechanical contact between the larger particles (Rh925) and cells deformed the microvilli of the FAE of the PPs, in contrast to the control group or to the smaller particles (Rh100), which smoothly dispersed between the microvilli (Supplementary figure 3). In addition, the expression of IgA on the surface of M cells increased after administration of the larger particles (Rh745 and Rh925) (enlarged parts in Figure 6E and F, arrowheads), in contrast to what was observed with the smaller particles (Rh100, Rh180, and Rh365) and the control group (Figure 6B–D, arrowheads). Moreover, larger particles (Rh925) (Figure 7C) increased IgA induction in the intestinal lumen more readily than the smaller particles (Rh100) (Figure 7B) or the control group (Figure 7A).

An increased number of CD11b$^+$ macrophages, 33D1$^+$ DCs, and IgA$^+$ cells in the SEDs of the PPs were observed after oral administration of the particles. Namely, the number of CD11b$^+$ macrophages that contained smaller particles (Rh100, Rh180, and Rh365) in the SEDs of the PPs was greater (Figure 3B–D, arrowheads) than that of the control group (Figure 3A, arrowheads). The ratios of CD11b$^+$ macrophages

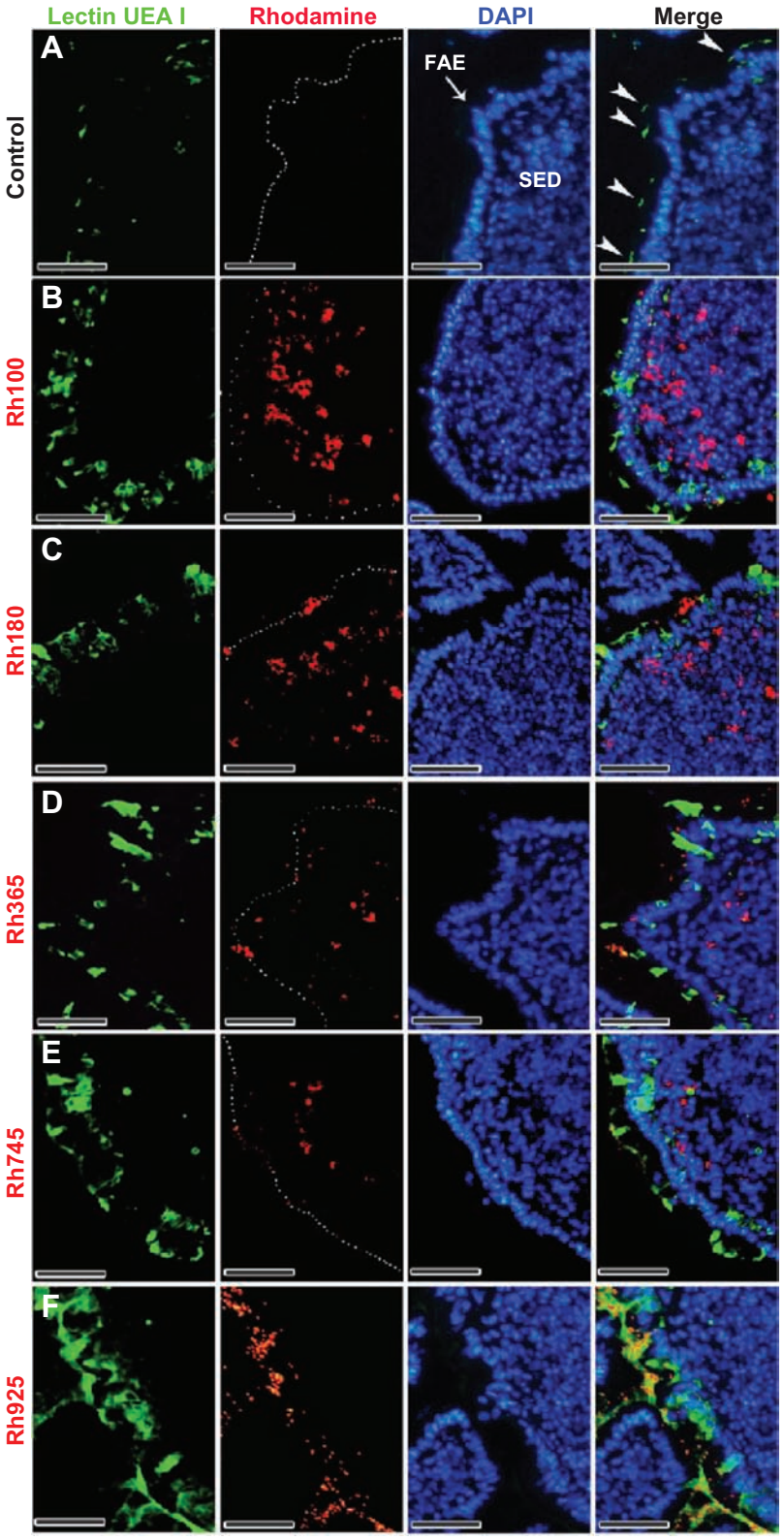

Figure 2 Fluorescent microscope images showing the FAE of PPs that had been stained with lectin UEA I (a marker for alpha-L-fucose residue on M cells) after 4 hours of oral administration of different sizes of fluorescent thiol-organosilica particles. (**A**) Control, M cells were scattered in the FAE, and alpha-L-fucose residue was expressed on the surface and upper cytoplasm of M cells. PP after administration of (**B**) Rh100 particles, (**C**) Rh180 particles, (**D**) Rh365 particles, (**E**) Rh745 particles, and (**F**) Rh925 particles. The expression of alpha-L-fucose residue on the surface and cytoplasm of M cells increased more in animals that had been administered Rh745 or Rh925 than in animals that had been administered the smaller particles Rh100, Rh180, or Rh365 or the control.

Note: Scale bar = 50 μm.

Abbreviations: FAE, follicle-associated epithelium; PPs, Peyer's patches; Rh, rhodamine B; SED, subepithelial dome; UEA I, *Ulex europaeus* agglutinin I.

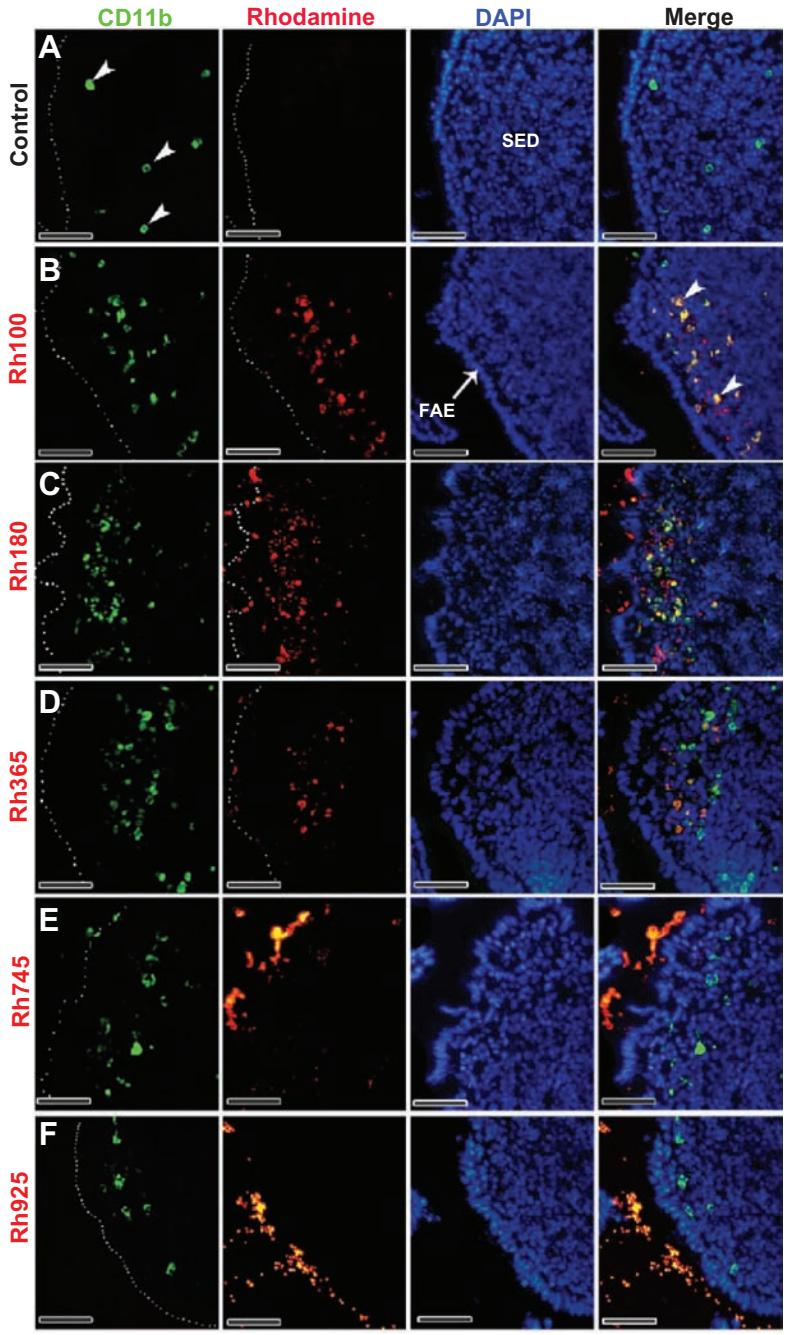

Figure 3 Fluorescent microscope images showing the SED of PPs stained with CD11b (Mac 1α chain) antibody (CD11b) (a marker for macrophages) after 4 hours of oral administration of different sizes of fluorescent thiol-organosilica particles. (**A**) Control, macrophages scattered in the SEDs of PPs. PPs after administration of (**B**) Rh100 particles, (**C**) Rh180 particles, and (**D**) Rh365 particles; there was co-localization of particles and $Cd11b^+$ macrophages, and the number of $CD11b^+$ macrophages increased compared with the control. PPs after administration of (**E**) Rh745 particles and (**F**) Rh925 particles; the number of $CD11b^+$ macrophages were similar to that of the control. $CD11b^+$ macrophages aggregated under the FAE of PPs after administration of all particle sizes.
Note: Scale bar = 50 μm.
Abbreviations: FAE, follicle associated epithelium; PPs, Peyer's patches; Rh, rhodamine B; SED, subepithelial dome.

that contained Rh100 or Rh180 particles to those without particles were higher than the corresponding ratio calculated with $CD11b^+$ macrophages that contained Rh365 particles. Furthermore, the number of $CD11b^+$ macrophages in the SEDs of PPs after administration of the larger particles (Rh745 and Rh925) was similar or slightly higher (Figure 3E and F) than that of the control group. The uptake of smaller particles (Rh100) by PPs induced $CD11b^+$ macrophages to migrate under the FAE of PPs (Figure 5A, arrowheads); and similar to $CD11b^+$ macrophages, the uptake of smaller particles (Rh100, Rh180, and Rh365) (Figure 6B–D, arrowheads) increased the number of IgA^+ cells in the SEDs of PPs more

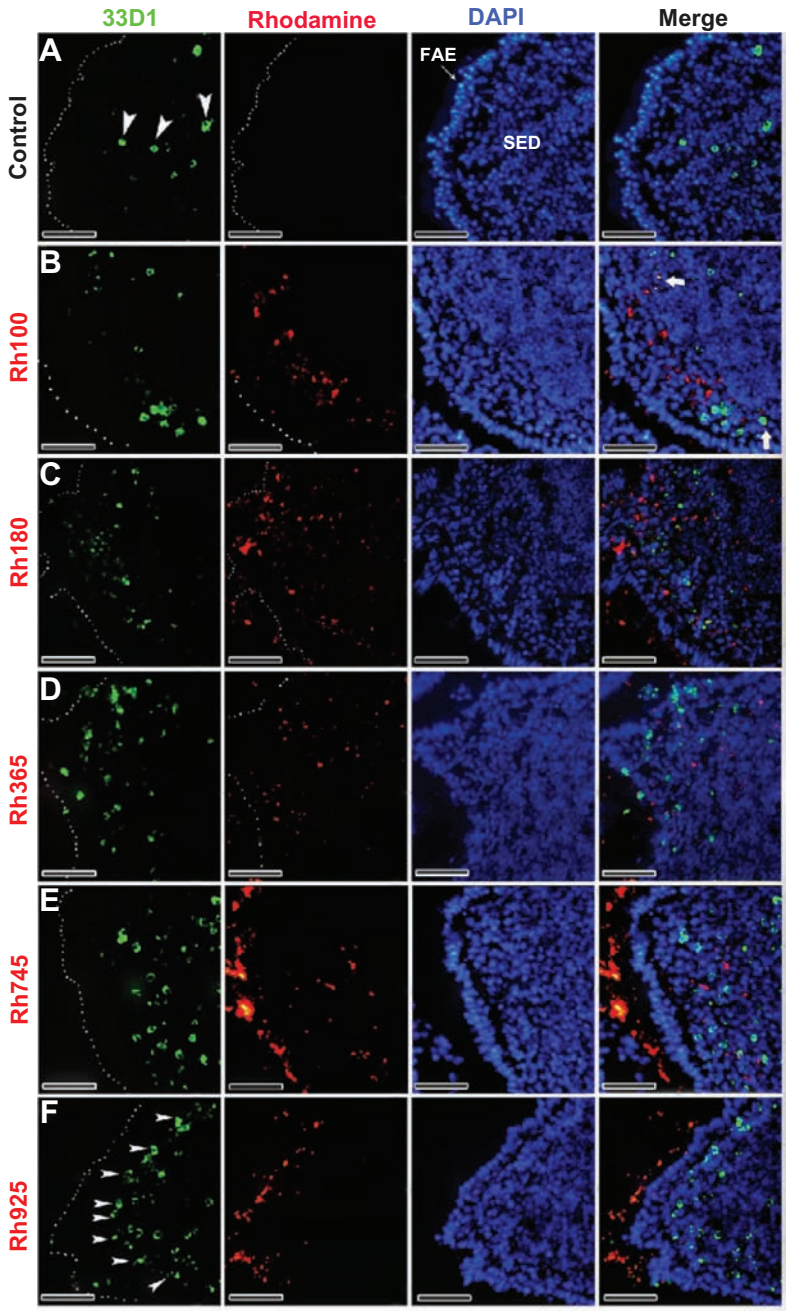

Figure 4 Fluorescent microscope images showing the SED of PPs stained with 33D1 antibody (a marker for DCs) after 4 hours of oral administration of differently sized fluorescent thiol-organosilica particles. (**A**) Control, 33D1$^+$ DCs scattered in the SED of the PPs. PPs after administration of (**B**) Rh100 particles, (**C**) Rh180 particles, and (**D**) Rh365 particles; there was no co-localization of particles and 33D1$^+$ DCs. The number of 33D1$^+$ DCs was similar to the control. PPs after administration of (**E**) Rh745 particles and (**F**) Rh925 particles; the number of 33D1$^+$ DCs increased when compared with the control. 33D1$^+$ DCs aggregated under the FAE of the PPs after administration of all particle sizes.
Note: Scale bar = 50 μm.
Abbreviations: DCs, dendritic cells; FAE, follicle associated epithelium; PPs, Peyer's patches; Rh, rhodamine B, SED, subepithelial dome.

readily than larger particles (Rh745 and Rh925) (Figure 6E and F) or the control group (Figure 6A). In contrast to CD11b$^+$ macrophages and IgA$^+$ cells, the mechanical contact of larger particles with the FAE of PPs (Rh745 and Rh925) increased the number of 33D1$^+$ DCs in the SEDs (Figure 4E and F, arrowheads), when compared with the control group (Figure 4A) or to the uptake of smaller particles (Rh100, Rh180, and Rh365) (Figure 4B–D, bold arrows). These data indicate that the uptake of smaller particles increases the number of CD11b$^+$ macrophages and IgA$^+$ cells. In contrast, the uptake and mechanical adhesion of larger particles increase the number of 33D1$^+$ DCs.

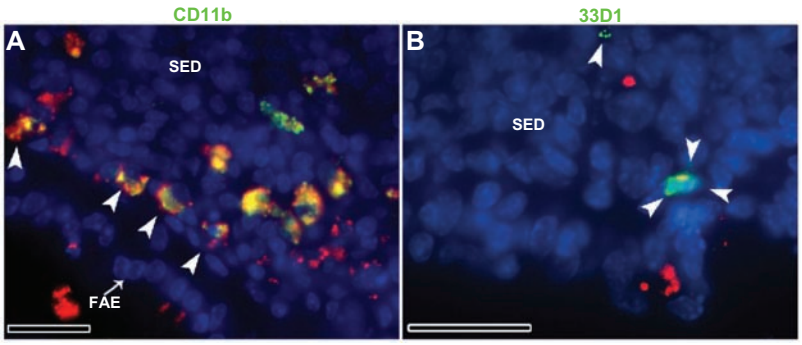

Figure 5 Fluorescent microscope images showing PPs at high magnifications after 4 hours of oral administration of Rh100 fluorescently labeled thiol-organosilica particles. (**A**) CD11b$^+$ macrophages containing particles scattered in the SED of the PPs and aggregated under the FAE of the PPs; large numbers of particles co-localized with CD11b$^+$ macrophages. **(B)** 33D1$^+$ DCs scattered in the SED of the PPs; there was little co-localization of the particles with 33D1$^+$ DCs.
Note: Scale bar = 25 μm.
Abbreviations: DCs, dendritic cells; FAE, follicle associated epithelium; PPs, Peyer's patches; Rh, rhodamine B; SED, subepithelial dome.

Quantitative analysis of the nanoimmunoresponse of immune cells of PPs after oral administration of thiol-organosilica particles

To evaluate and quantitatively compare the number of CD11b$^+$ macrophages, 33D1$^+$ DCs, and IgA$^+$ cells, the number of PP immune cells in the SEDs were counted and that number normalized to the average area (0.154 mm^2) (Figure 8). After administration of smaller particles (Rh100), the number of CD11b$^+$ macrophages in the SED of PPs was five times higher than that of the control group or two times higher than that of larger sized particles (Rh925). Furthermore, the number of IgA$^+$ cells after administration of smaller particles (Rh100) was seven times higher than that of control or four times higher than that of larger particles (Rh745 and Rh925). In contrast, the number of 33D1$^+$ DCs that accumulated after administration of larger particles (Rh925), within the same area, was two times higher than that of the control and other particle sizes. These quantitative data confirmed the immunohistochemical analysis of the nanoimmunoresponse of PP immune cells against thiol-organosilica particles.

Western blotting of the IgA nanoimmunoresponse after oral administration of thiol-organosilica particles

Because an increase in the number of IgA$^+$ cells was observed after oral administration of smaller particles, the protein level of IgA was measured by Western blotting using an anti-IgA antibody in bile, PP homogenates, and intestinal secretions. In Figure 9, it can be observed that Western blotting detected a band of 55 kDa, which is consistent with the molecular weight of IgA. In the bile sample (5 μg/lane), the intensity of the 55 kDa protein band after the administration of smaller or larger particles was significantly higher than that of the control group. Similarly, the intensity of the same protein band after administration of Rh100 was significantly higher than that after Rh925 administration (Figures 9A and 10). For PP homogenates (15 μg/lane), the intensity of the 55 kDa protein after Rh100 administration was higher than that of the control or after the administration of Rh925. Furthermore, after Rh925 administration, IgA levels were slightly higher or similar to that of the control group (Figures 9B and 10). In contrast, Western blotting analysis of intestinal secretions (10 μg/lane) indicated that the intensity of the 55 kDa protein after the administration of Rh925 was higher than that after the administration of Rh100, which, in turn, was slightly higher than that of the control group (Figures 9C and 10). These data revealed that IgA induction increased after a 4-hour administration of smaller particles (Rh100) in bile secretions and PP homogenates, when compared with the control group or the administration of larger particles (Rh925). In contrast, larger particles increased the induction of IgA in intestinal secretions, when compared with the control group or administration of smaller particles (Figure 10).

Discussion

In the present study, a mucosal, size-dependent nanoimmunoresponse, ie, a change in mouse PP immune cell numbers and expression of alpha-L-fucose and IgA secretion, using various sizes of thiol-organosilica particles was demonstrated. These results were unexpected because the particles were not immunologically functionalized. Although the smaller (Rh100) and larger (Rh925) particles were prepared from the same silica source, they showed different patterns of

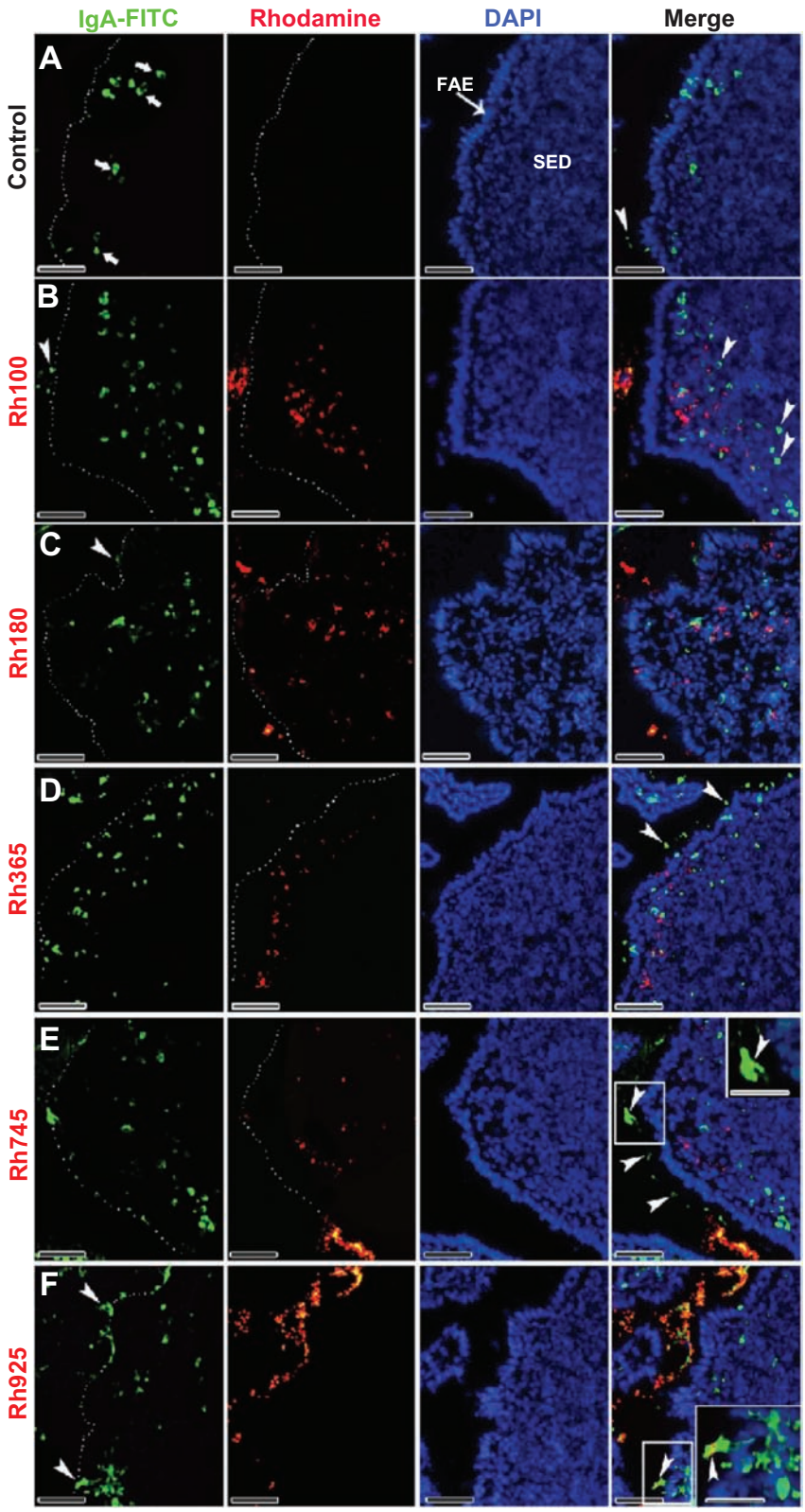

Figure 6 Fluorescent microscope images showing the SED of PPs stained with IgA antibody after 4 hours of oral administration of different sizes of fluorescently labeled thiol-organosilica particles. (**A**) Control, IgA^+ cells scattered in the SED of the PPs. PPs after administration of (**B**) Rh100 particles, (**C**) Rh180 particles, and (**D**) Rh365 particles; there was no co-localization of the particles and IgA^+ cells. The number of IgA^+ cells in animals treated with the smaller particles (Rh100, Rh180, and Rh365) increased compared with the control. PPs after administration of (**E**) Rh745 particles and (**F**) Rh925 particles; the number of IgA^+ cells were similar to that of the control, but IgA expression on the surface of M cells increased when compared with the smaller-sized particles or the control (white quadrates and enlarged parts of merged (**E**) and (**F**)).
Notes: Scale bar = (**A**–**F**), 50 μm; enlarged sections of merged (**E**) and (**F**), 10 μm.
Abbreviations: DCs, dendritic cells; FAE, follicle associated epithelium; IgA, immunoglobulin A; PPs, Peyer's patches; Rh, rhodamine B; SED, subepithelial dome.

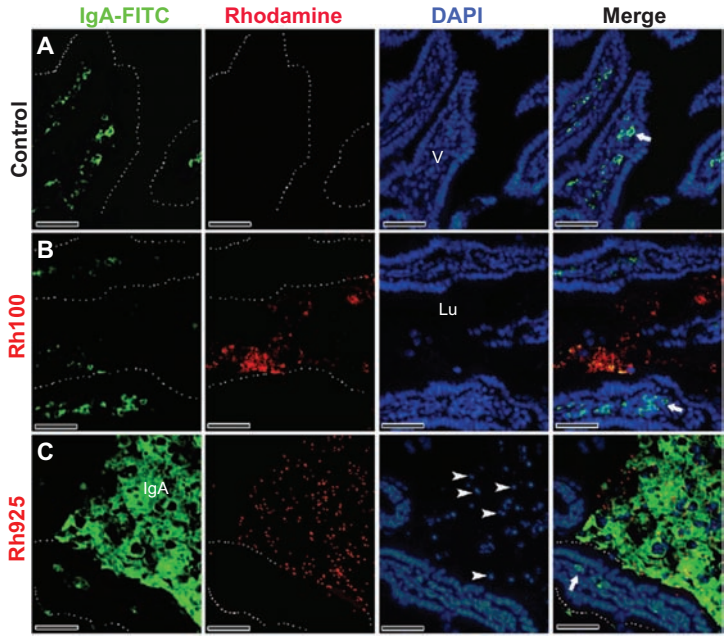

Figure 7 Fluorescent microscope images showing intestinal lumen (Lu) stained with IgA antibody after 4 hours of oral administration of fluorescently labeled Rh100 or Rh925 thiol-organosilica particles. (**A**) Control, IgA$^+$ cells (bold arrows) in the villi (V) lamina propria; and (**B**) Rh100 particles inside the intestinal lumen; no IgA expression inside the lumen was observed, similar to the control. (**C**) The Rh925 particles inside the intestinal lumen; IgA proteins that were secreted into the lumen and the leukocyte (arrow heads) number increased when compared with that of Rh100-administered animals.
Note: Scale bar = 50 μm.
Abbreviations: IgA, immunoglobulin A; Lu, lumen; Rh, rhodamine B; V, villi.

nanoimmunoresponse. In the present study, M cells of the PPs did not take up many of the larger particles (Rh925). Unlike the smaller particles, larger particles localized to the surface of the FAE of PPs and increased the amount of alpha-L-fucose residue and IgA expression on the surface of M cells. Additionally, the larger particles increased the numbers of 33D1$^+$ DCs more than the smaller particles. Alpha-L-fucose is an important cell surface carbohydrate and fucose-containing glycan, and it has important roles in host-microbe interactions.[34] Also, IgA has an important role in the humoral immune response against pathogens and antigen-coated NPs,[22–24] and in the mouse intestine, IgA was found to bind selectively to M cells of the PPs.[35,36] Therefore, the authors of this present study conclude that larger particles can stimulate the mucosal nanoimmunoresponse.

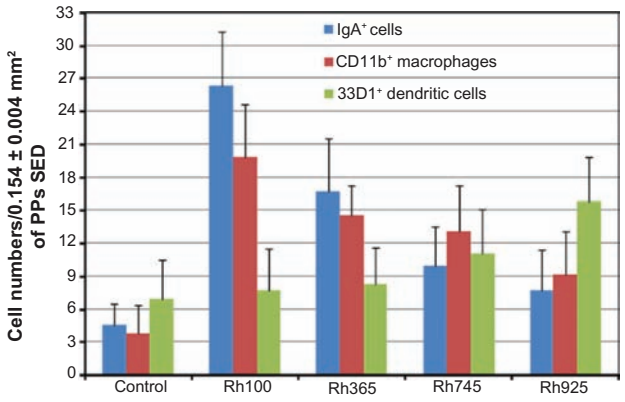

Figure 8 Quantitative analysis of the nanoimmunoresponse of immune cells from PPs 4 hours after oral administration of different-sized, fluorescently labeled, thiol-organosilica particles. Immune cells of PPs were counted in 0.154 ± 0.004 mm^2 sections of the SEDs of PPs. The uptake of smaller particles (Rh100) increased the number of CD11b$^+$ macrophages and IgA$^+$ cells two- and fourfold, respectively, when compared with larger particles (Rh925) or five- and sevenfold, respectively, when compared with the control. In contrast, mechanical adhesion of larger particles increased the number of 33D1$^+$ DCs twofold when compared with smaller particles or the control.
Note: Bars represented means ± standard deviations (n = 20).
Abbreviations: DCs, dendritic cells; IgA, immunoglobulin A; PPs, Peyer's patches; Rh, rhodamine B; SED, subepithelial dome.

Larger particles that are similar in size to bacteria or spores have stronger surface tension forces and heavier and higher gravitational effects than smaller particles;[37] therefore, these particles might induce mechanotransduction in the FAE of PPs. Previous studies have revealed that mechanotransduction is a physiological process that allows cells to sense and respond to mechanical stress,[38] and several molecules and receptors that have intermediary roles in mechanotransduction have been identified.[3,39–46] One of these receptors is the Toll-like receptor-2 (TLR2),[42,43] which is expressed on the villus epithelium and on the FAE and in M cells of PPs. This receptor plays a critical role in the early, innate immunoresponse and invasion of pathogens by sensing microorganisms.[3,45–49] Furthermore, the TLR2 induces B-cell homing to the gastrointestinal tract and IgA production.[48,49]

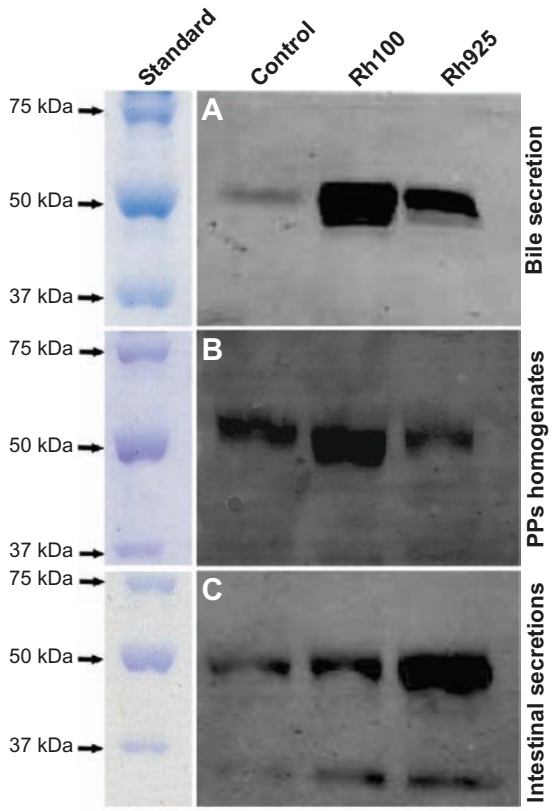

Figure 9 Western blotting analysis of IgA induction after 4 hours of oral administration of Rh100 or Rh925 particles. Western blotting analysis of IgA induction in (**A**) the bile (5 μg/each lane), (**B**) the intestinal secretions (10 μg/each lane), and (**C**) in PP homogenates (15 μg/each lane). Smaller thiol-organosilica particles (Rh100) induced IgA in both PP homogenates and bile secretions when compared with larger particles (Rh925); however, the opposite was true for intestinal secretions.
Abbreviations: IgA, immunoglobulin A; PPs, Peyer's patches; Rh, rhodamine B.

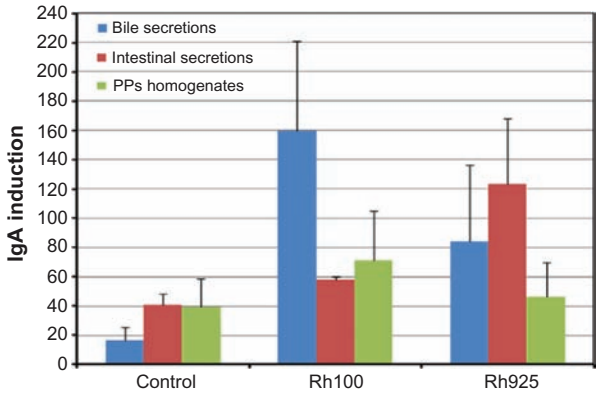

Figure 10 Densitometric analysis of IgA induction in the bile, intestinal secretions and PP homogenates after 4 hours of oral administration of Rh100 or Rh925 particles.
Note: Bars represent means ± standard deviations (n = 4).
Abbreviations: IgA, immunoglobulin A; PPs, Peyer's patches; Rh, rhodamine B.

Therefore, it is possible that the adhesion of larger particles to the FAE stimulates mechanotransduction receptors, such as the TLR2, which then induce mucosal nanoimmunoresponses such as IgA and M cell alpha-L-fucose.

DCs play a primary role in oral tolerance and defense against mucosal pathogens,[8] by maintaining IgA production and regulating the activity of T, B, and plasma cells.[8,15,16] An increased number of 33D1$^+$ DCs in the SEDs of PPs was observed when larger particles were administrated; however, there was no direct contact between the larger particles and DCs. It was reported that enterocytes in the FAE of PPs could release chemokines that attract DCs,[50–52] and one of the chemokines was the macrophage inflammatory protein (MIP-3 alpha), which was expressed by the FAE of PPs and attracted DCs into the SEDs of those PPs.[50] Therefore, it is possible that larger particles increase the number of 33D1$^+$ DCs by releasing chemokines that are produced in the FAE. However, no report describing the induction of chemokines by mechanotransduction has been published. The authors of this present paper hypothesize that mechanotransduction due to larger particles induces the release of chemokines from the FAE, and those chemokines attract 33D1$^+$ DCs into the SEDs of PPs.

In this study, it was demonstrated that, smaller thiol-organosilica particles were taken up mainly by CD11b$^+$ macrophages rather than by 33D1$^+$ DCs. In contrast to these findings, a previous study reported that orally administrated, hydrophobic, fluorescent polystyrene particles (200 nm), were taken up mainly by CD11c$^+$ DCs rather than by CD11b$^+$ macrophages.[4] Also, previously it was reported that, if the surface charge of the NPs is positive or uncharged, it has an affinity for adsorptive enterocytes through hydrophobic interactions, whereas a negatively charged and hydrophilic surface shows greater affinity for adsorptive enterocytes and M cells.[32,53] It is possible that this difference in cellular uptake was brought about by the surface properties of the particles, eg, thiol-organosilica particles are hydrophilic and naturally possess mercaptopropyl residues that contain alkyl chains and thiol residues with highly negative surface charges (Figure 1A). Therefore, the particles could have adsorbed antigenic molecules that were derived from commensal microbes in the intestinal lumen, which could explain why thiol-organosilica particles have an increased ability to bind proteins, as reported previously.[28] Therefore, orally administered, smaller particles could be significantly taken up by CD11b$^+$ macrophages from PPs, rather than by 33D1$^+$ DCs, but further studies are needed to clarify the mechanism of uptake of thiol-organosilica particles by PP cells.

The present study demonstrated that the uptake of smaller particles increased the number of CD11b$^+$ macrophages and IgA$^+$ cells in the SEDs of PPs, and this uptake was dependent on the size of the particle. In contrast, after the administration

Table 2 A summary of the size-dependent co-localization of thiol-organosilica particles and the immune cells from PPs.

	Thiol-organosilica particles localization with PP immune cells				PP immune cells number change			M cell molecules expression change		IgA induction		
	UEA I$^+$ M cells	CD11b$^+$ macrophages	33D1$^+$ DCs	IgA$^+$ cells	CD11b$^+$ macrophages	33D1$^+$ DCs	IgA$^+$ cells	α-L-fucose residue	IgA	PP homogenates	Intestinal secretion around PP	Bile secretion
Control	–	–	–	–	+	+	+	+	±	±	±	+
Rh100	++	+++*	+	–	+++*	±*	+++*	++	+	+++	++	+++*
Rh180	++	+++	+	–	+++	±*	+++	++	+	×	×	×
Rh365	++	++	–	–	++	++	++	++	+	×	×	×
Rh745	+++	++	–	–	++	++	++	++	++	×	×	×
Rh925	+++	+	–	–	±*	+++	±*	+++	+*	++	+*	++

Notes: The nanoimmunoresponse of PP: immune cell numbers change, the expression of some molecules in PP M cell changes, and IgA is induced after administration of several sizes of thiol-organosilica particles. + = frequency value as compared with the control value, – = zero value, x = no supported data, * = significant value.

Abbreviations: IgA, immunoglobulin A; PPs, Peyer's patches; Rh, rhodamine B; UEA I, *Ulex europaeus* agglutinin I.

of larger particles, the number of CD11b$^+$ macrophages and IgA$^+$ cells was similar to that of the control cells. Macrophages have an important role in the uptake and clearing of nanomaterials and pathogens from the body,[54–56] and it has been reported that after oral administration of the *Scrapie* virus, the uptake of the virus and the number of Mac-3$^+$ macrophages increased in the SEDs of the PPs.[14] IgA$^+$ cells function in the small intestine to enhance the immune system against some infections by producing IgA. In a previous study, when mice were orally administered *Lactobacillus paracasei* subsp,[9] or *reovirus* (70–80 nm in diameter), IgA$^+$ cells increased in number in the SEDs of the PPs and villi lamina propria.[57] In the present authors' previous work, size-dependent uptake of particles by the M cells of PPs was reported, and this uptake was achieved by transcytosis of PPs M cells and enterocytes and a paracellular pathway in the FAE of PPs. The uptake of six different sizes of particles by M cells of PPs using simultaneous, dual administration was also compared, and it was found that the uptake of the smaller particles by immune cells of the PPs was higher than that of the larger particles.[32] Smaller particles were easily transported to the SED of PPs, and the presence of more of the smaller particles in the SED increased the number of CD11b$^+$ macrophages and IgA$^+$ cells. In that study, the size-dependent nanoimmunoresponse that alters the number of CD11b$^+$ macrophages and IgA$^+$ cells in the SEDs of PPs were described, and the results indicate that smaller particles enter into PPs easily via three pathways,[32] and could increase the number of CD11b$^+$ macrophages and IgA$^+$ cells with respect to the number of particles that are taken up. However, larger particles, which are transported to PPs inefficiently, do not increase the number of immune CD11b$^+$ macrophages and IgA$^+$ cells in the PPs.

In this present study, an increase in IgA secretion in bile and PP homogenates after the administration of smaller particles (Rh100) was observed. Recently, some studies reported a size-dependent nanoimmunoresponse in serum after oral administration of various sizes of surface-functionalized particles.[22–24,58] An increase in serum IgA and IgG was observed after the administration of 500 or 100 nm tetanus toxoid-loaded PLGA NPs but not after 1 μm NPs or tetanus toxoid solution alone.[23] It has also been reported that serum IgG induction by ovalbumin PLGA microspheres show the following dependence on particle size: 4.0 μm > 1.3 μm = 7.5 μm > 14 μm. Also, particle surface area may be the most appropriate parameter to evaluate the pulmonary inflammatory potential.[58] The size-dependent nanoimmuneresponse and pulmonary inflammation come from the larger surface area of smaller particles as compared with larger particles.[24,58] These reports

indicated that inductions of serum IgA and IgG by orally administering particles depended not only on the size of the particles but also on the type of particle, antigen, and surface area. In this present study, the adhesion of larger particles to the FAE of PPs increased mucosal IgA secretion and IgA expression on the surface of M cells; however, the uptake of smaller particles by the SED of PPs increased systemic IgA in bile and PP homogenates 4 hours after oral administration. These results allow us to hypothesize that there are two routes of size-dependent IgA nanoimmunoresponse in the small intestine, from enterohepatic circulation into lumen (enterohepatic route) and directly via mucosal membrane into the lumen (mucosal route) (Figure 1A). In the enterohepatic route, many macrophages take up commensal antigens from the intestinal lumen and process and present antigenic information to B and plasma cells. As reported previously, smaller particles can be taken up by PPs through PP M cells as well as two novel pathways (through PP enterocytes and between PP enterocytes). The smaller particles were taken up by PPs more, as compared with larger particles.[32] Smaller particles with higher surface area as compared with larger particles, probably introduce more antigenic molecules into the SED of PPs or other lymphoid tissues such as villi lamina propria. A portion of the IgA is released, binds to the IgA receptor on epithelial cells, and is transported into the intestinal lumen. The other portion of IgA that is produced in the lymphoid tissues enters the portal flow, is transported into the liver, and then released into the bile.[59,60] This mechanism could explain the induction of IgA by smaller particles via enterohepatic route. In the mucosal route, larger particles mechanically stimulate the FAE, including M cells, and IgA molecules are released from M cells and are then secreted into the lumen directly. In this report, the authors proposed two possible routes, enterohepatic route and mucosal route, of two size-dependent of IgA secretion into the intestine lumen using organosilica particles.

Conclusion

Size-dependent nanoimmunoresponses in PPs were demonstrated by orally administering various sizes of thiol-organosilica particles to mice. As shown in Table 2, larger particles (745 and 925 nm) increased the expression of alpha-L-fucose on the surface of M cells of the FAE and the secretion of mucosal IgA into the intestinal lumen. In addition, larger particles increased the number of $33D1^+$ DCs in the SED of PPs. Smaller particles (100, 180, and 365 nm) were transported to the SED and taken up by $CD11b^+$ macrophages, which then increased in number and increased the content of systemic IgA in both PP homogenates and bile. The novel findings in this study indicated that there are two size-dependent routes of IgA secretions into the intestinal lumen: the mucosal route by larger particles and the enterohepaic route by smaller particles. However, the mechanisms for size-dependent enhancement of the immunological responses of thiol-organosilica particles must be clarified. Additionally, in this study, size-dependent nanoimmunoresponse after 4 hours of oral administration was evaluated. The nanoimmunoresponse may be altered with time, and further studies, such as those on the time-dependent change in IgA induction after administration, are required to understand the mucosal and systemic nanoimmunoresponse enhancement that occurs when using thiol-organosilica particles. Furthermore, an investigation of the enhancement of the size-dependent nanoimmunoresponse and its mechanism are important for the development of nanomedicine, mucosal vaccination enhancement, and protective immunity.

Acknowledgments

This work was supported in part by a Grant-in-Aid for Younger Scientists (No 17790356) (to M Nakamura) and a Grant-in-Aid for Scientific Research (C) (Nos 19510117 and 21500409) (to M Nakamura) from the Ministry of Education, Science, Sports, and Culture of Japan as well as a Grant for Practical Application of University R&D Results under the Matching Fund Method (to M Nakamura) from the New Energy and Industrial Technology Development Organization (NEDO) of Japan. Financial support of the Egyptian Ministry of Higher Education and Scientific Research, Missions Sector (to A Awaad) is gratefully acknowledged.

Disclosure

The authors report no conflicts of interest in this work.

References

1. Salman HH, Irache JM, Gamazo C. Immunoadjuvant capacity of flagellin and mannosamine-coated poly(anhydride) nanoparticles in oral vaccination. *Vaccine*. 2009;27(35):4784–4790.
2. Salman HH, Gamazo C, Agüeros M, Irache JM. Bioadhesive capacity and immunoadjuvant properties of thiamine-coated nanoparticles. *Vaccine*. 2007;25(48):8123–8132.
3. Chabot S, Wagner JS, Farrant S, Neutra MR. TLRs regulate the gatekeeping functions of the intestinal follicle-associated epithelium. *J Immun*. 2006:176(7):4275–4283.
4. Shreedhar VK, Kelsall BL, Neutra MR. Cholera toxin induces migration of dendritic cells from the subepithelial dome region to T- and B-Cell areas of Peyer's patches. *Infec Immun*. 2003;71(1):504–509.
5. Semete B, Booysen LI, Kalombo L, et al. In vivo uptake and acute immune response to orally administered chitosan and PEG coated PLGA nanoparticles. *Toxicol Appl Pharmacol*. 2010;249(2):158–165.

6. Kaewamatawong T, Shimada A, Okajima M, et al. Acute and subacute pulmonary toxicity of low dose of ultrafine colloidal silica particles in mice after intratracheal instillation. *Toxicol Path*. 2006;34(7):958–965.
7. Sen D, Deerinck TJ, Ellisman MH, Parker I, Cahalan MD. Quantum dots for tracking dendritic cells and priming an immune response in vitro and in vivo. *PLoS ONE*. 2008;3(9):e3290.
8. Johansson C, Kelsall BL. Phenotype and function of intestinal dendritic cells. *Semin Immun*. 2005;17(4):284–294.
9. Tsai YT, Cheng PC, Liao JW, Pan TM. Effect of the administration of Lactobacillus paracasei subsp. paracasei NTU 101 on Peyer's patch-mediated mucosal immunity. *Int Immunopharmacol*. 2010;10(7):792–798.
10. Gonzalez MJ, Plummer EM, Rae CS, Manchester M. Interaction of Cowpea Mosaic virus (CPMV) nanoparticles with antigen presenting cells in vitro and in vivo. *PLoS ONE*. 2009;4(11):e7981.
11. Zuercher AW, Cebra JJ. Structural and functional differences between putative mucosal inductive sites of the rat. *Eur J Immunol*. 2002;32(11):3191–3196.
12. Romero-Trevejo JL, Gómez-Villamandos JC, Pedrera M, Blanco A, Bautista MJ, Sánchez-Cordón PJ. Immunohistochemical study of macrophage and cytokine dynamics in the gut of scrapie-infected mice. *Histol Histopathol*. 2010;25(8):1025–1038.
13. Umesaki Y, Okada Y, Imaoka A, Setoyama H, Matsumoto M. Interactions between epithelial cells and bacteria, normal and pathogenic. *Science*. 1997;276(5314):964–965.
14. Jeong GN, Jo UB, Ryu HY, KimYS, Song KS, Yu IJ. Histochemical study of intestinal mucins after administration of silver nanoparticles in Sprague–Dawley rats. *Arch Toxicol*. 2010;84(1):63–69.
15. Macpherson AJ, Uhr T. Induction of protective IgA by intestinal dendritic cells carrying commensal bacteria. *Science*. 2004;303(5664):1662–1665.
16. Tezuka H, Abe Y, Iwata M, et al. Regulation of IgA production by naturally occurring TNF/iNOS-producing dendritic cells. *Nature*. 2007;448(7156):929–933.
17. Magistris MTD. Mucosal delivery of vaccine antigens and its advantages in pediatrics. *Adv Drug Del Rev*. 2006;58(1):52–67.
18. Mishra N, Tiwari S, Vaidya B, Agrawal GP, Vyas SP. Lectin anchored PLGA nanoparticles for oral mucosal immunization against hepatitis B. *J Drug Target*. 2010;19(1):1–12.
19. He X, Wang F, Jiang L, Li J, Liu S, Xiao Z. Induction of mucosal and systemic immune response by single-dose oral immunization with biodegradable microparticles containing DNA encoding HBsAg. *J Gen Virol*. 2005;86(Pt 3):601–610.
20. Akagi T, Ueno M, Hiraishi K, Baba M, Akashi M. AIDS vaccine: Intranasal immunization using inactivated HIV-1-capturing core-corona type polymeric nanospheres. *J Control Release*. 2005;109(1–3):49–61.
21. Gupta PN, Mahor S, Rawat A, Khatri K, Goyal A, Vyas SP. Lectin anchored stabilized biodegradable nanoparticles for oral immunization. 1. Development and in vitro evaluation. *Int J Pharm*. 2006;318(1–2):163–173.
22. Nagamoto T, Hattori Y, Takayama K, Maitani Y. Novel chitosan particles and chitosan-coated emulsions inducing immune response via intranasal vaccine delivery. *Pharm Res*. 2004;21(4):671–674.
23. Jung T, Kamm W, Breitenbach A, Hungerer K, Hundt E, Kisse T. Tetanus toxoid loaded nanoparticles from sulfobutylated poly(vinyl alcohol)-graft-poly(lactide-co-glycolide): evaluation of antibody response after oral and nasal application in mice. *Pharm Res*. 2001;18(3):3352–3360.
24. Takahiro U, Shigeru G. Oral delivery of poly(lactide-co-glycolide) microspheres containing ovalbumin as vaccine formulation: particle size study. *Bio Pharm Bull*. 1994;17(9):1272–1276.
25. Thomas C, Gupta V, Ahsan F. Influence of surface charge of PLGA particles of recombinant hepatitis B surface antigen in enhancing systemic and mucosal immune responses. *Int J Pharm*. 2009;379(1):41–50.
26. Nakamura M, Ishimura K. Synthesis and characterization of organosilica nanoparticles prepared from 3-mercaptopropyltrimethoxysilane as the single silica source. *J Phys Chem C*. 2007;111(51):18892–18898.
27. Nakamura M, Ishimura K. One-pot synthesis and characterization of three kinds of thiol-organosilica nanoparticles. *Langmuir*. 2008;24(9):5099–5108.
28. Nakamura M, Ozaki S, Abe M, Doi H, Matsumoto T, Ishimura K. Size-controlled synthesis, surface functionalization, and biological applications of thiol-organosilica particles. *Colloids Surf B Biointerfaces*. 2010;79(1):19–26.
29. Nakamura M, Ishimura K. Size-controlled, one-pot synthesis, characterization, and biological applications of epoxy-organosilica particles possessing positive zeta potential. *Langmuir*. 2008;24(21):12228–12234.
30. Nakamura M, Ozaki S, Abe M, Matsumoto T, Ishimura K. One-pot synthesis and characterization of dual fluorescent thiol-organosilica nanoparticles as non-photoblinking quantum dots and their applications for biological imaging. *J Mater Chem*. 2011;21(12):4689–4695.
31. Hayashi K, Nakamura M, Ishimura K. In situ synthesis and photoresponsive rupture of organosilica nanocapsules. *Chem Commun (Camb)*. 2011;47(5):1518–1520.
32. Awaad A, Nakamura M, Ishimura M. Imaging of size-dependent uptake and identification of novel pathways in mouse Peyer's patches using fluorescent organosilica particles. *Nanomedicine*. Epub September 1, 2011.
33. Irmukhametova GS, Mun GA, Khutoryanskiy VV. Thiolated mucoadhesive and PEGylated nonmucoadhesive organosilica nanoparticles from 3-mercaptopropyltrimethoxysilane. *Langmuir*. 2011;(15):9551–9556.
34. Becker DJ, Lowe JB. Fucose: biosynthesis and biological function in mammals. *Glycobiology*. 2003;13(7):41R–53R.
35. Mantis NJ, Cheung MC, Chintalacharuvu KR, Rey J, Corthésy B, Neutra MR. Selective adherence of IgA to murine Peyer's patch M cells: Evidence for a novel IgA receptor. *J Immun*. 2002;169(4):1844–1851.
36. Weltzin R, Lucia-Jandris P, Michetti P, Fields BN, Kraehenbuhl JP, Neutra MR. Binding and transepithelial transport of immunoglobulins by intestinal M cells: demonstration using monoclonal IgA antibodies against enteric viral proteins. *J Cell Biol*. 1989;108(5):1673–1685.
37. Mijailovich SM, Kojic M, Tsuda A. Particle-induced indentation of the alveolar epithelium caused by surface tension forces. *J Appl Physiol*. 2010;109(4):1179–1194.
38. Khan KM, Scott A. Mechanotherapy: how physical therapists' prescription of exercise promotes tissue repair. *Br J Sports Med*. 2009;43(4):247–252.
39. Schwartz MA, DeSimone DW. Cell adhesion receptors in mechanotransduction. *Curr Opin Cell Biol*. 2008;20(5):551–556.
40. Wang Y, Maciejewski BS, Drouillard D, et al. A role for caveolin-1 in mechanotransduction of fetal type II epithelial cells. *Am J Physiol Lung Cell Mol Physiol*. 2010;298(6):L775–L783.
41. Imai Y, Kondoh S, Kato S. Mechanotransduction via estrogen receptors in bone. *Clin Calcium*. 2008;18(9):1272–1277.
42. Kim HG, Kim JY, Gim MG, Lee JM, Chung DK. Mechanical stress induces tumor necrosis factor-α production through $Ca2^{+}$ release-dependent TLR2 signaling. *Am J Physiol Cell Physiol*. 2008;295(2):C432–C439.
43. Geiger B, Spatz JP, Bershadsky AD. Environmental sensing through focal adhesions. *Nat Rev Mol Cell Biol*. 2009;10(1):21–33.
44. Zhang X, Shephard F, Kim HB, et al. TILRR, a novel IL-1RI co-receptor, potentiates MyD88 recruitment to control Ras-dependent amplification of NF-kappaB. *J Biol Chem*. 2010;285(10):7222–7232.
45. Tohno M, Shimosato T, Kitazawa H, et al. Toll-like receptor 2 is expressed on the intestinal M cells in swine. *Biochem Biophys Res Commun*. 2005;330(2):547–554.
46. Shimosato T, Tohno M, Kitazawa H, et al. Toll-like receptor 9 is expressed on follicle-associated epithelia containing M cells in swine Peyer's patches. *Immunol Lett*. 2005;98(1):83–89.
47. Chow WL, Lee YK. Free fucose is a danger signal to human intestinal epithelial cells. *Br J Nutr*. 2008;99(3):449–454.

48. Liang Y, Hasturk H, Elliot J, et al. Toll-like receptor 2 induces mucosal homing receptor expression and IgA production by human B cells. *Clin Immunol*. 2011;138(1):33–40.
49. He B, Xu W, Santini PA, et al. Intestinal bacteria trigger T cell-independent immunoglobulin A(2) class switching by inducing epithelial-cell secretion of the cytokine APRIL. *Immunity*. 2007;26(6):812–826.
50. Iwasaki A, Kelsall BL. Localization of distinct Peyer's patch dendritic cell subsets and their recruitment by chemokines macrophage inflammatory protein (MIP)-3α, MIP-3β, and secondary lymphoid organ chemokine. *J Exp Med*. 2000;191(8):1381–1394.
51. Zhao X, Sato A, Dela Cruz CS, et al. CCL9 is secreted by the follicle-associated epithelium and recruits dome region Peyer's patch $CD11b^+$ dendritic cells. *J Immunol*. 2003;171(6):2797–2803.
52. Cook DN, Prosser DM, Forster R, et al. CCR6 mediates dendritic cell localization, lymphocyte homeostasis, and immune responses in mucosal tissue. *Immunity*. 2000;12(5):495–503.
53. Jani P, Halbert GW, Langridge J, Florence AT. The uptake and translocation of latex nanospheres and microspheres after oral administration to rats. *J Pharm Pharmacol*. 1989;4(12):809–812.
54. Pron B, Boumaila C, Jaubert F, et al. Dendritic cells are early cellular targets of Listeria monocytogenes after intestinal delivery and are involved in bacterial spread in the host. *Cell Microbiol*. 2001;3(5):331–340.
55. Maignien T, Shakweh M, Calvo Pet, et al. Role of gut macrophages in mice orally contaminated with scrapie or BSE. *Int J Pharm*. 2005;298(2):293–304.
56. Geiser M, Baumann M, Cruz-Orive LM, Im Hof V, Waber U, Gehr P. The effect of particle inhalation on macrophage number and phagocytic activity in the intrapulmonary conducting airways of hamsters. *Am J Respir Cell Mol Biol*. 1994;10:594–603.
57. Major AS, Cuff CF. Enhanced mucosal and systemic immune responses to intestinal reovirus infection in beta2-microglobulin-deficient mice. *J Virol*. 1997;71:5782–5789.
58. Stoeger T, Reinhard C, Takenaka S, et al. Instillation of six different ultrafine carbon particles indicates a surface area threshold dose for acute lung inflammation in mice. *Environ Health Perspect*. 2006;114(3):328–333.
59. Zho F, Neutra MR. Antigen delivery to mucosa-associated lymphoid tissues using liposomesas a carrier. *Biosci Rep*. 2002;22(2):355–369.
60. Bos NA, Jiang HQ, Cebra JJ. T cell control of the gut IgA response against commensal bacteria. *Gut*. 2001;48(6):762–764.

Supplementary figures

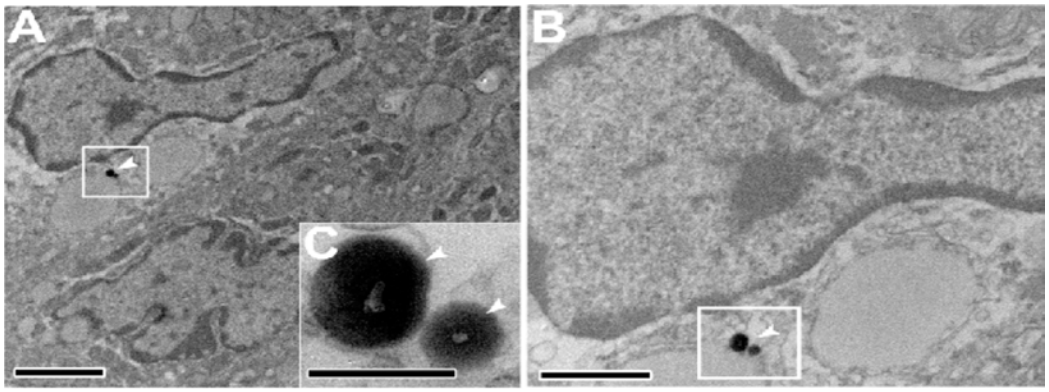

Figure S1 Electron photomicrographs showing the colocalization of Rh130 thiol-organosilica particles and PP SED cells.
Note: Scale bar = (**A**) 2 μm; (**B**) 1 μm; (**C**) 200 nm.
Abbreviations: PPs, Peyer's patches; Rh, rhodamine B; SED, subepithelial dome.

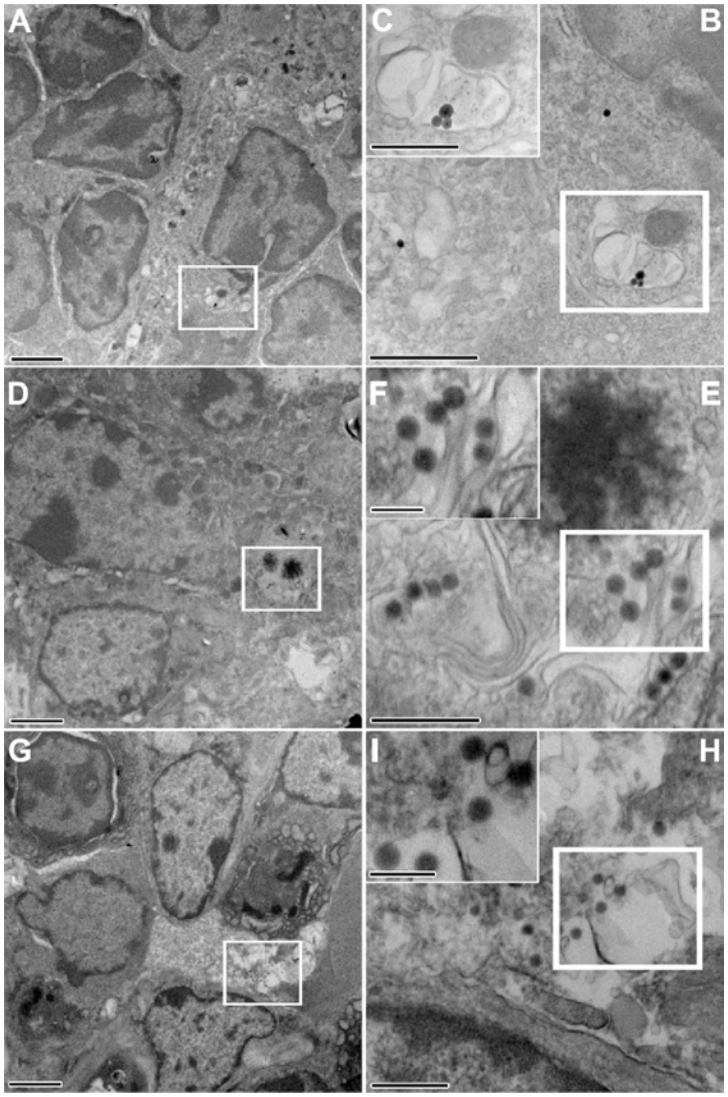

Figure S2 Electron photomicrographs showing, (**A–E**) The colocalization of Rh130 particles with PP SED cells. (**G** and **H**) The diffusion of Rh130 thiol-organosilica particles between the PP SED cells.
Note: Scale bar = (**A**), (**D**), (**G**), 2 μm; (**B**), 1 μm; (**E**), (**H**), 500 nm; (**C**), (**F**), (**I**) 200 nm.
Abbreviations: PPs, Peyer's patches; Rh, rhodamine B; SED, subepithelial dome.

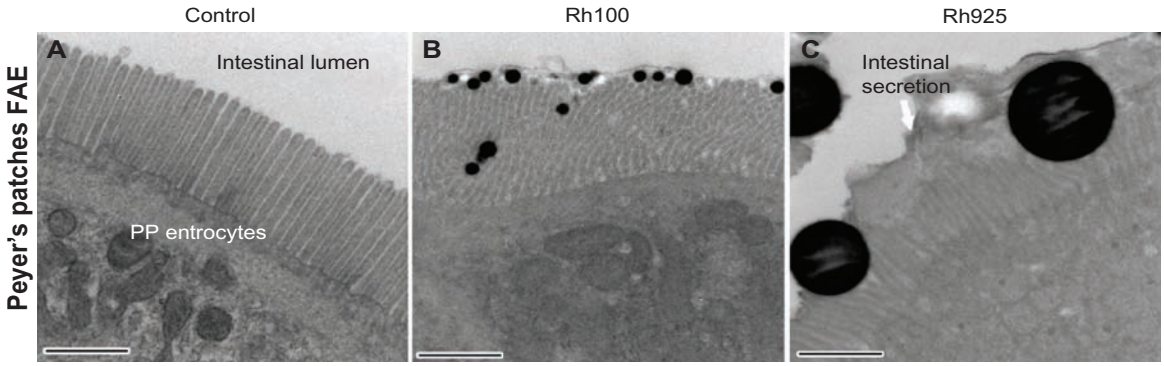

Figure S3 Electron photomicrographs showing the PP FAE enterocytes and the mechanical adhesion of thiol-organosilica particles. (**A**) The control of PP FAE, (**B**) mechanical adhesion of Rh100 on PP FAE, (**C**) mechanical adhesion of Rh925 on PP FAE.
Note: Scale bar = (**A**); (**B**); and (**C**), 700 nm.
Abbreviations: FAE, follicle associated epithelium; PPs, Peyer's patches; Rh, rhodamine B.